13B.6 STEPPED FREQUENCY MICROWAVE RADIOMETER ALGORITHM IMPROVEMENTS ADDRESSING RAIN CONTAMINATION OF SURFACE WIND SPEED MEASUREMENTS IN TROPICAL CYCLONES

Bradley W. Klotz[1, 2] and Eric W. Uhlhorn[2]
[1] University of Miami/RSMAS/CIMAS, Miami, Florida*
[2] NOAA/AOML/HRD, Miami, Florida†

1. INTRODUCTION

Improving forecasts of tropical cyclones (TCs) has become increasingly important because of increased public awareness. Tropical forecasters use a variety of tools to create their predictions, most of which rely on observation platforms to provide important information. Whether it is through direct interpretation or through interpretation of numerical models that utilize these observations, the information must be reliable to produce a valid forecast. According to DeMaria et al. (2005) and subsequently Elsberry et al. (2007) with verification from Aberson (2008), official model intensity forecasts since 1990 improved by as much as 15% at 72 hours but not quite as much at 24 and 48 hours.

One possible way to continue the improvements of TC forecasts, especially intensity, either through direct observation or model interpretation is to improve the observations platforms upon which these methods rely. A particular platform that has become of more interest to TC community over the last decade is the Stepped Frequency Microwave Radiometer (SFMR), which is flown on aircraft to produce surface wind speeds and rain rates. The SFMR is capable of providing real-time data from the storm to the Tropical Prediction Center/National Hurricane Center (TPC/NHC) in order to help forecasters make informed decisions.

The SFMR made its first observations during Hurricane Allen in 1980 (Jones et al. 1981, Black and Swift 1984). Since that time, the SFMR has gone through several development phases and has been a part of NOAA's Hurricane Research Division (HRD) data archive since 1999 (Jiang et al. 2006, http://www.aoml.noaa.gov/hrd/data_sub/hurr.html).
While the SFMR is an enhancement to aircraft reconnaissance of TCs, no instrument is perfect. With the addition of the SFMR to the Air Force (USAF) Reserve 53rd Reconnaissance Wing aircrafts in 2007, there have been some noticeable issues with wind speed retrievals from the instrument.

* *Corresponding author address*: Bradley W. Klotz, Univ. of Miami, RSMAS/CIMAS, 4600 Rickenbacker Causeway, Miami, FL 33149-1098; email: brad.klotz@noaa.gov

† *Corresponding author address*: Eric W. Uhlhorn, NOAA/AOML, Hurricane Research Division, 4301 Rickenbacker Causeway, Miami, FL 33149; email: eric.uhlhorn@noaa.gov

One issue of particular interest is the SFMR producing higher than expected wind speeds in conditions of moderate to heavy rain. For example, SFMR have reported 55 - 60 kt winds when buoys near the same location reported wind speeds of 35 kts during heavy rain. While this may not happen in every circumstance, there is a definite problem that needs addressing. A new model for the SFMR is developed in the hopes of solving this issue and making the data more reliable to forecasters.

2. DATA

NOAA WP-3D aircraft are flown in TC investigation missions every hurricane season to collect various atmospheric and sea surface data. For the purpose of this work, the main sources of data come from the SFMR and the GPS dropwindsondes that are launched during these flights. The SFMR collects brightness temperatures (T_B) at six frequencies ranging from 4.74 to 7.09 GHz and passes these T_B to a radiative transfer model to estimate surface wind speeds and rain rates. Sampling rate of all six brightness temperatures is one Hertz with independent results sampled every 0.1 Hz (Uhlhorn and Black, 2003). For more detailed information about the development and algorithm specifics of the current SFMR instrument, consult Uhlhorn and Black (2003).

GPS dropwindsondes are periodically released during missions into TCs, collecting information about horizontal wind speed, temperature, relative humidity, and pressure. Wind speeds are sampled at a rate of two Hertz, allowing for a vertical resolution of approximately five meters (Uhlhorn et al. 2007). Hock and Franklin (1999) discuss, in detail, some of the specifics related to the GPS dropwindsondes.

SFMR and GPS dropwindsonde data for this study are taken from two WP-3D aircraft from the 2005-2009 Atlantic hurricane seasons. These aircraft are identified as N42RF and N43RF, respectively. Over 400 SFMR-GPS sonde pairs are created from these data and are used to evaluate the wind-emissivity function of the SFMR algorithm. These pairs will also be used to evaluate differences between the current model (CM) wind speeds against those of the new Uhlhorn-Klotz model (UKM) wind speeds.

3. METHODS

Finding a solution to address the issue of overestimation of surface wind speeds from the SFMR involves techniques that were used in past work, especially Uhlhorn and Black (2003) and Uhlhorn et al. (2007). To look at specific methods, this section is broken into three sub-sections for clarification and explanation.

3.1 A New Rain Model

Past work with the rain model led to a frequency component that was too dependent on rain rate. Because this model produces rain rate estimates with a degree of uncertainty and because the wind model depends upon the rain model, the rain dependence is believed to have a negative impact (i.e. overestimation) on the wind model within high rain rate circumstances. By weakening this dependence, these negative influences are expected to be lessened, producing more realistic wind speeds in the presence of heavy rain. The current rain model takes the form:

$$\kappa_r = aR^b, \quad (1)$$

where κ_r is the absorption due to rain, R is rain rate, b is 1.15, and a is given as

$$a = gf^{n(R)}. \quad (2)$$

Here, g is 1.87 X 10^{-6} Np km^{-1}, f is frequency, and $n(R)$ is $2.6R^{0.0736}$. In the rain portion of the UKM, the same form as (1) and (2) is followed, but b is 0.823, g is 5.877 X 10^{-6} Np km^{-1}, and $n(R)$ is 2.981, thus weakening a's frequency dependence on rain. These new coefficients were empirically determined by taking the brightness temperatures from a test flight in September 2009 and creating a new κ - R relationship through use of a Precipitation Imaging Probe (PIP). These results are presented in a companion poster.

3.2 A Matching Wind Model

To get an accurate wind model, the wind speeds from the GPS dropwindsondes are paired with the emissivities that are determined from the SFMR brightness temperatures. For this pairing, wind speeds from the 150 m height (referred to as WL150) taken from the TEMPDROP messages sent from the aircraft are matched with the corresponding emissivities. The WL150 winds must be converted to surface winds through a reduction factor that is given in Franklin et al. (2003). Uhlhorn et al. (2007) mention that this reduction was specifically used in eyewall estimations but show no reason that it cannot be used for weaker wind speeds. Once the pairs are created, outliers are removed using one standard deviation of the population. It is from this population that new coefficients to the wind-emissivity model can be empirically derived. The model follows the following form:

$$\begin{aligned} \varepsilon_w &= a_1 U_{sfc}, \ U_{sfc} \le w_l \\ &= a_2 + a_3 U_{sfc} + a_4 U_{sfc}^2, \ w_l < U_{sfc} \le w_u \\ &= a_5 + a_6 U_{sfc}, \ U_{sfc} > w_u \ , \end{aligned}$$

where w_l = 7 m s^{-1} , w_u is the location of the upper connection point between the top two pieces of the model, a_n are the fitted coefficients to the model, and U_{sfc} is the surface-adjusted wind speed taken from the WL150 reduction factor. The upper connection point is determined by testing values for w_u between 20 and 40 m s^{-1} and then finding the value that produces the lowest root mean squared difference over the entire piece-wise fit. For the CM, the values for a_n and w_u are

$$\begin{aligned} (a_1, a_2, a_3, a_4, a_5, a_6) = (&0.0401, 0.2853, \\ &-0.0418, 0.0058, \\ &-5.6658, 0.3317) \text{ X } 10^{-2} \end{aligned}$$
$$w_u = 31.9 \text{ m s}^{-1}.$$

After recalculating the emissivities with the UKM rain model in place, new coefficients were found for the best fit and are provided as follows

$$\begin{aligned} (a_1, a_2, a_3, a_4, a_5, a_6) = (&0.0593, 0.2309, \\ &-0.0067, 0.0047, \\ &-4.5648, 0.2940) \text{ X } 10^{-2} \end{aligned}$$
$$w_u = 31.9 \text{ m s}^{-1}.$$

This new wind-emissivity model was then tested in conjunction with the new rain model to determine differences with the CM.

4. RESULTS AND DISCUSSION

With a new potential model in place to help remove the overestimation of surface winds during heavy rain, some statistical tests are performed on the two models for all flights used and for specific cases. The following sections provide some results of these analyses.

4.1 UKM and CM comparison

Running the SFMR algorithm under the current settings and proposed settings produced some interesting differences. In certain conditions, the model does not converge to a solution, thus producing an error or no solution. One simple aspect to compare between the two models is the ratio of determined solutions to undetermined solutions that are produced when running the algorithm. A higher ratio of solutions indicates better performance from the model. Table 1 shows the ratios and some difference statistics for all flights and then for each aircraft.

Table 1. Mean ratio of T_B producing solutions to those that do not produce solutions. Also displayed are mean and median differences between the UKM and the CM for all flights and for each NOAA P-3.

	All flights	N43RF	N42RF
UKM ratio	30.1:1	20.2:1	52.6:1
CM ratio	16.3:1	9.7:1	31.2:1
Mean Δ (UKM – CM)	771	888	502
Median Δ	409	398	430
% UKM improvement	+3.4	+4.1	+2.1

The mean ratio for all flights for the UKM shows that there are nearly twice as many solutions per one undetermined solution than results for the CM. This result implies that the UKM is improving upon the CM in that more solutions are produced on the whole. With the median and mean differences for all flights, there are a substantially higher number of solutions per flight for

the UKM. According to Table 1, this is actually about a 3.4% improvement upon the CM on average. The two aircraft provide slightly different results, but they are of the same order of magnitude. These results give reason to be optimistic about the output from the UKM.

Because the UKM produces more solutions, it is likely that there is some variability in the wind speeds and rain rates between the two models. To start the model comparisons, it is important to see how the wind-emissivity functions match with each other. Figure 1 displays the CM and UKM wind-emissivity functions, providing a visual difference between the two.

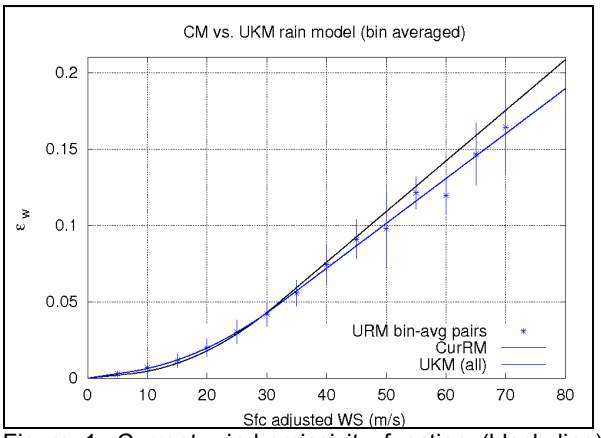

Figure 1. Current wind-emissivity function (black line) plotted in comparison with the UKM wind-emissivity function (blue line). The UKM function was determined from a 5 m s^{-1} bin-average of the SFMR-dropwindsonde pairs. Blue asterisks indicate the SFMR-sonde bin-averaged pairs.

It is clear to see that with the UKM rain model in place, the emissivities are slightly larger than the CM emissivities at low and moderate wind speeds. As the wind speeds approach and surpass hurricane strength, the emissivities become weaker than those of the CM. The main objective is to reduce the effect of rain on wind speed, especially during heavy rain, which is listed as 10 mm hr^{-1} < RR < 60 mm hr^{-1} (Glickman 2000). Therefore, it is expected that the absorption due to rain should be less than what the CM produces. From the relationship between absorption and transmittance (Uhlhorn and Black, 2003), emissivity should decrease with increasing transmittance. Because the absorption and emission are directly related, Fig. 1 shows that with decreased emissivity above 25 m s^{-1} the absorption (κ) due to rain is effectively decreasing, and transmittance effectively increases. It is then concluded that the UKM reduces the absorption due to rain, thus reducing the wind speed in moderate to heavier rain conditions.

Because the UKM rain model correctly decreases the emissivity, it has already been stated that the wind speeds will likely be reduced in the presence of increasing rain rate. Figure 2 shows the bin-averaged difference between the UKM and CM in 10 mm hr^{-1} bins.

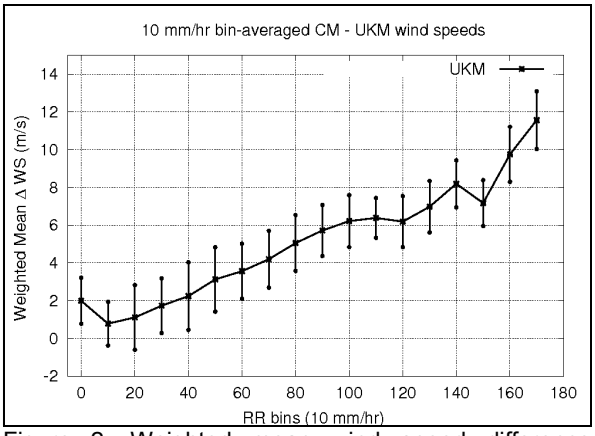

Figure 2. Weighted mean wind speed differences displayed in bin-averages of 10 mm hr^{-1} are shown for CM – UKM. The vertical, black lines indicate the errors in these bin-averages and are taken from the standard deviation of each bin.

According to Fig. 2, wind speeds are reduced between 0.78 – 3.56 ± 1.16 – 1.79 m s^{-1} at rain rates up to 60 mm hr^{-1}. Wind speed differences within this range increase steadily as rain rate increases. Between 60 and 150 mm hr^{-1}, the wind speeds do not increase quite as rapidly even though there is still an increase in the difference between the two models. Here the wind speed differences range from 3.56 – 8.20 ± 1.05 – 1.51 m s^{-1}. The range considered here is between 60 and 150 mm hr^{-1} because the number of instances of rain rates above 150 mm hr^{-1} is small enough to skew the wind speed differences. If the average slopes of these ranges are compared, the lower rain rate range has a slope of 0.06 whereas the higher rain rate range has a slope of 0.04, indicating a slight weakening of the rate of increase.

Another way to view how the wind speeds change with changing rain rate is to create bins of wind speed and bins of rain rate and calculate the weighted mean wind speed differences within those bin ranges. Figure 3 displays this information.

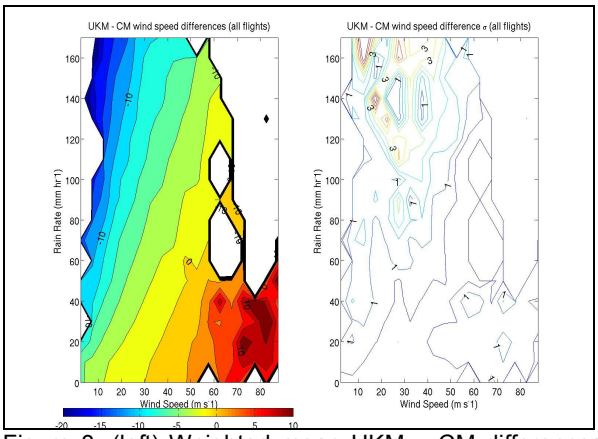

Figure 3. (left) Weighted mean UKM – CM differences per wind speed (5 m s^{-1}) and rain rate bins (10 mm hr^{-1}). Contours are every 2 m s^{-1} difference in wind speed with "colder" colors indicating larger negative differences. Contours are labeled every 10 m s^{-1}. Areas of white represent missing data. (right) Standard deviations of

the wind speed differences (per wind speed and rain rate bin) at contour intervals of 0.5 m s^{-1} with labels every 2 m s^{-1}. Both panels display all data from 2005 – 2009.

When examining Fig. 3, it is clear to see that at high wind speed bins (> 60 m s^{-1}) and low rain rate bins (< 30 mm hr^{-1}), the UKM wind speeds tend to be higher than the CM wind speeds on the order of 4 – 10 ± 0 – 1 m s^{-1}. In the opposite circumstance (low wind speed, high rain rate), the UKM wind speeds are less than the CM wind speeds on the order of 12 – 16 ± 2 – 4 m s^{-1}. It should also be noted that in these regions, there are very few data points (< ~15 bin^{-1}), which would leave one to believe that the wind speed differences in this range are questionable. One key result that Figure 3 displays is that in the region of question for this work (wind speeds between 20 – 50 m s^{-1} and rain rates between 60 – 120 mm hr^{-1}), UKM wind speeds are reduced on the order of 0 – 8 ± 0 – 2 m s^{-1}. Obviously if the rain rate increases, the wind speed difference increases slightly, and the opposite is true for decreasing rain rate.

4.2 UKM/CM and dropwindsonde comparisons

Another way that model differences can be checked is by comparing the models against the dropwindsonde surface-adjusted wind speeds (U_{sfc} or U_s). A certain amount of bias should be detected in these comparisons. Student's t-tests will indicate whether these biases are statistically significant. Figure 4 shows the disagreement the two models have with each other. Tables 2 and 3 provide the mean biases and Student's t-test for all flights and for each aircraft.

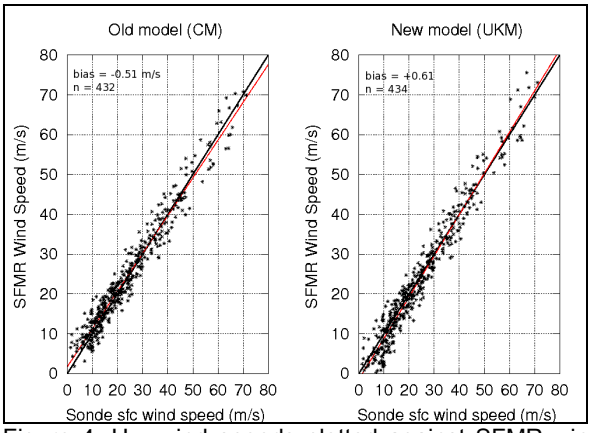

Figure 4. U_{sfc} wind speeds plotted against SFMR wind speeds from all flights. The mean bias is indicated along with the number of pairs in the upper left of each frame. Black (red) lines indicate the 1:1 (best-fit) lines.

Table 2. Mean biases and Student's t-test results for the GPS – CM dropwindsonde pairs.

	Bias (GPS-CM, m s^{-1})	p value	95% significant?
All flights	-0.51	0.599	No
N43RF	-0.21	0.842	No
N42RF	-1.93	0.296	No

Table 3. Same as Table 2 but for GPS – UKM dropwindsonde pairs.

	Bias (GPS-UKM, m s^{-1})	p value	95% significant?
All flights	+0.61	0.546	No
N43RF	+0.84	0.456	No
N42RF	-0.30	0.876	No

The relationship between model and sonde wind speeds as seen in Fig. 4 has a larger bias for all flights in the UKM comparison. However, this may be slightly higher because of the disparities above 50 m s^{-1}. The Student's t-test p-values for the UKM describe the difference with the dropwindsondes as not significant at a 95% confidence interval. This result implies that the populations do not vary enough to produce different means, which is a positive result. The t-tests for the CM indicate no statistical significance, meaning that these wind speeds also compare similarly to the GPS dropwindsondes. While the UKM wind speeds are improved during rainy conditions, it appears as though they do not provide a substantial improvement with the dropwindsonde surface-adjusted wind speeds.

The relationship of the models to the dropwindsondes and to each other can also be checked by using normalized, de-trended cumulative distribution functions with corresponding Kolmogorov–Smirnov tests. With these comparisons, information about the distribution relationships is given. Figures 5 and 6 along with Table 4 visualize these relationships.

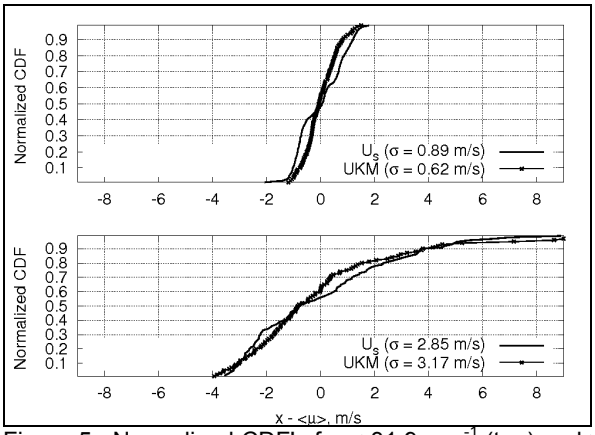

Figure 5. Normalized CDF's for < 31.9 m s^{-1} (top) and ≥ 31.9 m s^{-1} (bottom) for UKM-GPS comparison.

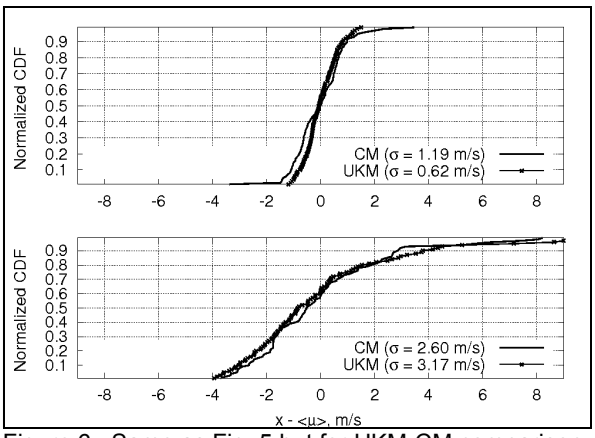

Figure 6. Same as Fig. 5 but for UKM-CM comparison.

Table 4. Normalized CDF standard deviations and Kolmogorov–Smirnov ('KS') test results for all flights and for NOAA 43. Test statistics are indicated as statistically significant (SS) and not statistically significant (NSS) at 95%.

	All Flights	N43RF
GPS σ (< 31.9 m s^{-1})	0.89	0.73
GPS σ (≥ 31.9 m s^{-1})	2.85	2.66
CM σ (< 31.9 m s^{-1})	1.19	1.05
CM σ (≥ 31.9 m s^{-1})	2.60	2.32
UKM σ (< 31.9 m s^{-1})	0.62	0.59
UKM σ (≥ 31.9 m s^{-1})	3.17	2.80
GPS p val (< 31.9 m s^{-1})	0.02 (SS)	0.26 (NSS)
GPS p val (≥ 31.9 m s^{-1})	0.34 (NSS)	0.89 (NSS)
CM p val (< 31.9 m s^{-1})	0.07 (NSS)	0.34 (NSS)
CM p val (≥ 31.9 m s^{-1})	0.67 (NSS)	0.44 (NSS)

Comparing the UKM wind speeds to the dropwindsonde wind speeds through the use of the normalized, de-trended CDF's in Fig. 5 and Table 4 shows that the UKM has less spread at lower wind speeds (< 31.9 m s^{-1}) but greater spread at higher wind speeds (≥ 31.9 m s^{-1}) according to the standard deviations. Because of these differences in standard deviation at the lower wind speeds and because of the Kolmogorov-Smirnov tests, the GPS dropwindsonde distribution has more variability than the UKM distribution. This variability in distributions is statistically significant as well. Slightly different results exist for the CM and UKM comparison. Differences in the standard deviations of the lower wind speeds are slightly larger for this comparison, indicating more spread and more variability for the CM. However, the Kolmogorov-Smirnov test indicates that these are differences are not statistically significant. At the higher winds, the UKM has slightly more variability but these differences are also not statistically significant.

4.3 UKM and CM differences – case studies

Knowing that the statistical analyses provide evidence that the UKM improves upon the CM calculations of wind speeds and rain rates, it is important to see how these models compare when directly examining individual flights. There are several cases during the 2005-2009 hurricane seasons that provide excellent examples of how the differences seen in section 4.1 would be seen in a single flight. Three cases are shown below and include a leg during the 1 September 2007 Hurricane Felix flight, a leg from the 19 August 2009 Hurricane Bill flight, and a leg from a 21 September 2009 test flight over the Gulf of Mexico.

4.3.1 Hurricane Felix case

Hurricane Felix developed east of the Caribbean Sea and tracked steadily to the west-northwest until making landfall in Nicaragua on 4 September, 2007 (Beven 2008). NOAA operated 5 flights into Hurricane Felix between 31 August – 3 September, and the leg under consideration for this case was during the flight that Felix was declared a hurricane by NHC. Figure 7 below shows this leg that begins 2 hours and 50 minutes into the flight.

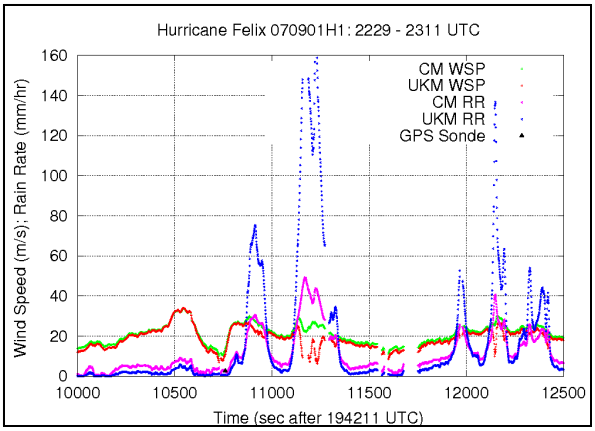

Figure 7. Flight leg of NOAA 42 into Hurricane Felix on 1 September 2007. Red (green) crosses and blue (magenta) asterisks indicate UKM (CM) SFMR wind speeds and rain rates, respectively. Time is referred to as seconds after the start time of 19:42:11 UTC.

During this flight leg, the wind speeds remained below 40 m s^{-1}, but there were several rain rate spikes. The largest of these spikes appears about halfway through the leg, and wind speeds are reduced by approximately 10 m s^{-1}. The wind speed seems to mirror the tendencies of the rain rate in this instance and possibly is reduced too much. The rain rate spike just prior to the previously mentioned spike may provide a more realistic idea of what is expected of the UKM. The rain rate increases to almost 80 mm hr^{-1} and the wind speeds are reduced by 5 – 6 m s^{-1}. This case shows that the model is reducing the wind speeds in high rain rate situations, but it is possible that it is over-reducing under some conditions. In addition, it is obvious that the UKM and CM have extremely variable rain rates in comparison to one another, but this is to be expected due to the change that was made to the rain model mentioned in Section 3.

4.3.2 Hurricane Bill case

As one of the bright spots of the 2009 Atlantic hurricane season, Hurricane Bill developed over the open ocean and became a hurricane within two days of its formation (Avila 2009). Within 30 hours of being named, Bill increased in strength and became a major

hurricane as it began to curve to the northwest. This strength was maintained for nearly three days before Bill began to encounter stronger wind shear and cooler waters. NOAA operated six flights into Hurricane Bill between 18 – 20 August, and the leg under consideration here occurred during the second of the 19 August flights at which point Bill was a Category 4 hurricane.

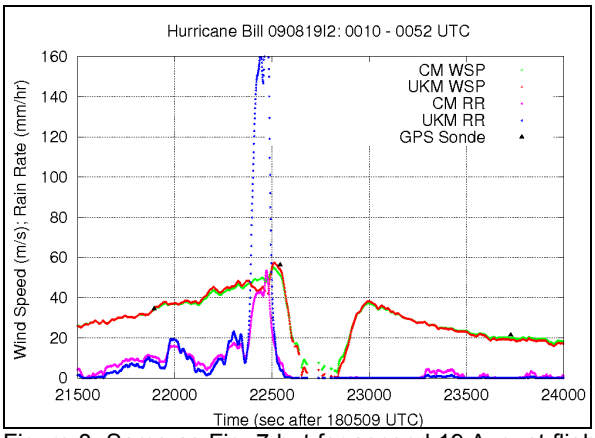

Figure 8. Same as Fig. 7 but for second 19 August flight into Hurricane Bill.

The leg under inspection shows an obvious pass through the eye of Bill. Several intriguing results are seen during this section of the flight, the most obvious of which is the spike in the rain rate to 160 mm hr^{-1} within the eyewall. Here the UKM wind speeds are reduced by nearly 8 m s^{-1}. Another observation is that in weaker rain rates (< 10 mm hr^{-1}), the wind speeds are within 0 – 2 m s^{-1} of each other. Even when there is no rain detected by the SFMR, the wind speeds remain within that 0 – 2 m s^{-1} window. It is clear to see from Fig. 8 that the UKM is able to maintain the correct wind speeds when the rain rate is weak while also decreasing the wind speed when the rain rate becomes heavy.

4.3.3 21 September 2009 Test Flight

With the previous cases, the UKM wind speeds and rain rates from two hurricanes were compared to those of the CM with somewhat encouraging results. A third, experimental case is now examined to see how the two model results compare under "semi-controlled" conditions. This experimental NOAA flight from 21 September was designed to fly through areas of isolated convection over the Eastern Gulf of Mexico to pinpoint locations of heavy rain within relatively and consistently weak environmental wind speeds (on the order of 0 – 10 m s^{-1}). Figure 9 provides some results from a portion of this flight.

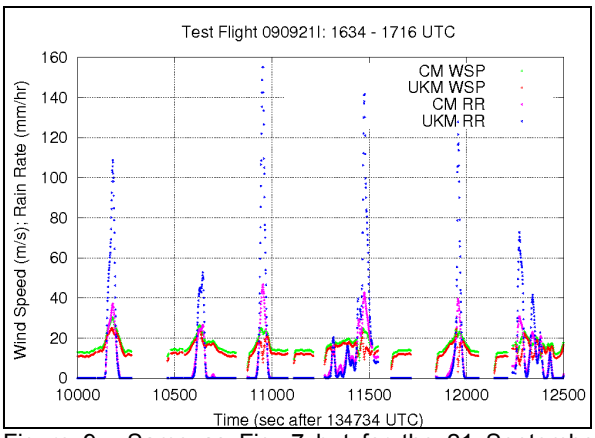

Figure 9. Same as Fig. 7 but for the 21 September 2009 test flight.

This type of experiment provides the ideal situation to evaluate the performance of the UKM. There were consistent spikes of heavy rain rate while the wind speeds before and after these spikes were within the desired range. Wind speeds increased during these spikes, but that is not totally unexpected due to the nature of convection (Aguado and Burt 2004). Similarly to the previous cases, the UKM wind speed reductions within these heavy rain spikes are anywhere from 5 – 10 m s^{-1}. During the larger rain rate spikes (> 120 mm hr^{-1}), some of the reductions are unrealistic because they drop more than 15 m s^{-1}. It is unnatural that the winds would drop by 15 m s^{-1} to values 2 – 3 m s^{-1} below the environmental wind speeds. As was shown previously in Fig. 3, these spikes fit into the region that is somewhat questionable, so the results are not totally unexpected. Another observation is the larger difference in the wind speeds (approximately 3 m s^{-1}) at very weak to no rain conditions. In the two hurricane cases, it was seen that the UKM was within 0 – 2 m s^{-1} of the CM under these similar conditions, but Fig. 3 also shows that the differences seen in Fig. 9 are within the realm of possibility. Keep in mind that the wind speeds and rain rates from the test flight were not included in the calculation of the results of Fig. 3, thus making them independent of those results.

5. CONCLUSIONS AND FUTURE WORK

The SFMR aboard the NOAA WP-3D aircraft and now the USAF WC-130J are vital for providing in-situ measurements of surface wind speeds and rain rates within potentially destructive TCs. Because the current SFMR algorithm has produced some incorrect wind speed results in the presence of heavy rain, a new model was derived to try to address this issue. SFMR data and GPS dropwindsonde data were taken from NOAA WP-3D flights during the 2005 – 2009 Atlantic hurricane seasons and were used to develop this new algorithm.

When comparing the current model (CM) with the new model (UKM), the UKM was able to double the amount of determinable solutions from the brightness temperatures observed by the SFMR. The number of solutions determined by the UKM was about 500 more than those found with the CM or an improvement of 3.4%. When comparing the models to the GPS

dropwindsondes, the biases found do not give reason to believe that the UKM wind speeds improve upon the relationship with the dropwindsondes. The CM bias was about -0.5 m s^{-1} while the UKM bias was 0.6 m s^{-1}, indicating that both models produce wind speeds within ~0.5 m s^{-1} of the dropwindsonde wind speed on average. However, the normalized CDF's of the CM and UKM wind speeds indicate that the UKM has less variability than the CM below 31.9 m s^{-1} and more variability than the CM above 31.9 m s^{-1}.

There are obvious differences between the two models, but numerically, the UKM wind speeds will tend to decrease more as the rain rate increases. Mean differences through binning of rain rates and wind speeds and rain rates combined both showed that within heavy rain conditions and moderate wind speeds, the UKM wind speeds are always reduced. The amount of reduction depends upon the strength of the rain, but the UKM successfully provides a reduction of the winds in heavy rain conditions. It is also important that the UKM does not significantly reduce or increase the wind speed in the presence of minimal or no rain. Even the individual cases that were examined showed that there were decreased wind speeds in the rainy areas and virtually unchanged wind speeds in the non-rainy areas.

While it is encouraging that the generally desired results were found, some of the reductions seemed too large, especially when the rain rates increased above the 120 mm hr^{-1} threshold. Granted this was not the case for all instances of rain rates above 120 mm hr^{-1} as was seen in the Hurricane Bill example. There also seems to be more variation at the weak rain rates and weak wind speeds as was seen from the test flight example. Because there is more spread in the differences at the extreme rain rates and during the calm conditions, some future analysis will be undertaken to examine possible reasons why this occurs and possible solutions to address these issues. The next step is to test this new algorithm in the field to find out how it behaves in real time. Hopefully, it will provide more reliable data to forecasters in the future.

REFERENCES

Aberson, S. D., 2008: An alternative tropical cylcone intensity forecast verification technique. *Wea. and Forecast.*, **23**, 1304-1310.

Aguado, E. and J. E. Burt, 2004: *Understanding Weather and Climate, Third Edition*. Pearson Education, Inc. 560 pp.

Avila, L., National Hurricane Center, cited 2009: Tropical Cyclone Report, Hurricane Bill (AL032009), 15 – 24 August 2009. [Available online at http://www.nhc.noaa.gov/pdf/TCR-AL032009_Bill.pdf].

Beven, J., National Hurricane Center, cited 2008: Tropical Cyclone Report, Hurricane Felix (AL062007), 31 August – 5 September 2007. [Available online at http://www.nhc.noaa.gov/pdf/TCR-AL062007_Felix.pdf].

Black, P. G. and C. T. Swift, 1984: Airborne Stepped Frequency Microwave Radiometer measurements of rainfall rate and surface wind speed in hurricanes. Preprints, *Second Conf. on Radar Meteorology*, Zurich, Switzerland, Amer. Meteor. Soc., 433 – 438.

DeMaria, M., M. Mainelli, L. K. Shay, J. A. Knaff, and J. Kaplan, 2005: Further improvements to the Statistical Hurricane Intensity Prediction Scheme (SHIPS). *Wea. and Forecast.*, **20**, 531 – 543.

Elsberry, R. L., T. D. B. Lambert, and M. A. Boothe, 2007: Accuracy of Atlantic and Eastern North Pacific Tropical Cyclone intensity forecast guidance. *Wea. and Forecast.*, **22**, 747 – 762.

Franklin, J. L., M. L. Black, and K. Valde, 2003: GPS dropwindsonde wind profiles in hurricanes and their operational implications. *Wea. and Forecast.*, **18**, 32 – 44.

Glickman, T. S. (Ed.), 2000: *American Meteorological Society Glossary of Meteorology, Second Edition*. Allen Press. 855 pp.

Hock, T. F. and J. L. Franklin, 1999: The NCAR GPS dropwindsonde. *Bull. Amer. Met. Soc.*, **80**, 407 – 420.

Jiang, H., P. G. Black, E. J. Zipser, F. D. Marks, Jr., and E. W. Uhlhorn, 2006: Validation of rain-rate estimation in hurricanes from the Stepped Frequency Microwave Radiometer: algorithm correction and error analysis. *J. Atmos. Sci.*, **63**, 252 – 267.

Jones, W. L., P. G. Black, V. E. Delnore, and C. T. Swift, 1981: Airborne microwave remote-sensing measurements of Hurricane Allen. *Science*, **214**, 274 – 280.

Uhlhorn, E. W. and P. G. Black, 2003: Verification of remotely sensed sea surface winds in hurricanes. *J. Atmos. And Ocean. Tech.*, **20**, 99 – 116.

_____, E. W., P. G. Black, J. L. Franklin, M. Goodberlet, J. Carswell, and A. S. Goldstein, 2007: Hurricane surface wind measurements from an operational Stepped Frequency Microwave Radiometer. *Mon. Wea. Rev.*, 135, 3070 – 3085.